

Structure, Energetics, and Dynamics of Water Adsorbed on the Muscovite (001) Surface: A Molecular Dynamics Simulation

Jianwei Wang,^{*,†,‡} Andrey G. Kalinichev,^{†,‡} R. James Kirkpatrick,^{†,‡} and Randall T. Cygan[§]

Department of Geology and NSF Water CAMPWS, University of Illinois at Urbana–Champaign, 1301 West Green Street, Urbana, Illinois 61801 and Geochemistry Department, Sandia National Laboratories, Albuquerque, New Mexico 87185

Received: October 14, 2004; In Final Form: June 21, 2005

Molecular dynamics (MD) computer simulations of liquid water adsorbed on the muscovite (001) surface provide a greatly increased, atomistically detailed understanding of surface-related effects on the spatial variation in the structural and orientational ordering, hydrogen bond (H-bond) organization, and local density of H₂O molecules at this important model phyllosilicate surface. MD simulations at constant temperature and volume (statistical *NVT* ensemble) were performed for a series of model systems consisting of a two-layer muscovite slab (representing 8 crystallographic surface unit cells of the substrate) and 0 to 319 adsorbed H₂O molecules, probing the atomistic structure and dynamics of surface aqueous films up to 3 nm in thickness. The results do not demonstrate a completely liquid-like behavior, as otherwise suggested from the interpretation of X-ray reflectivity measurements¹ and earlier Monte Carlo simulations.² Instead, a more structurally and orientationally restricted behavior of surface H₂O molecules is observed, and this structural ordering extends to larger distances from the surface than previously expected. Even at the largest surface water coverage studied, over 20% of H₂O molecules are associated with specific adsorption sites, and another 50% maintain strongly preferred orientations relative to the surface. This partially ordered structure is also different from the well-ordered 2-dimensional ice-like structure predicted by *ab initio* MD simulations for a system with a complete monolayer water coverage.³ However, consistent with these *ab initio* results, our simulations do predict that a full molecular monolayer surface water coverage represents a relatively stable surface structure in terms of the lowest diffusional mobility of H₂O molecules along the surface. Calculated energies of water adsorption are in good agreement with available experimental data.⁴

Introduction

Water adsorption on solid surfaces plays an important role in many natural and technological processes including mineral weathering, corrosion, water behavior in soils, pollutant transport in the environment, and heterogeneous ice nucleation. Thus, it has long been of widespread interest in many scientific fields from meteorology and geochemistry to heterogeneous catalysis and materials chemistry.^{5–10} The adsorption of water can change the properties of mineral surfaces, including the protonation state, surface structure and charge, surface energy, and surface reactivity.^{5,11} In parallel, the properties of water near mineral surfaces are strongly influenced by substrate structure and composition.^{5,12} Important molecular scale questions about such water sorption are the nature of adsorption (molecular vs dissociative), the local structural and energetic characteristics of the adsorption sites, the nature and strength of the bonding between water and the substrate, the local structure and orientation of the adsorbed water molecules, the extended structure of the first few molecular layers of adsorbed water, and the thermodynamic and transport properties in these layers as a function of the film thickness.¹³ In this paper, we present

a computational molecular dynamics (MD) study of the interaction of water with the muscovite (001) surface that addresses many of these questions in relation to this prototypical mineral surface.⁹

Muscovite is a layered dioctahedral aluminosilicate with the chemical formula $\text{KAl}_2(\text{Si}_3\text{Al})\text{O}_{10}(\text{OH})_2$.¹⁴ It is a popular choice for many interfacial experiments because its perfect (001) cleavage allows creation of large areas of smooth surface on the atomic scale. However, despite intensive experimental and computational studies of the interaction of water with the muscovite (001) surface, there are many remaining uncertainties concerning the molecular scale structure, dynamics, and energetics of the adsorbed water.^{1–4,12,15–18}

The muscovite (001) surface exposes the basal oxygens of the six-member (Si,Al) rings of the tetrahedral sheet. Substitution of one Al for one of every four Si in this sheet causes a net negative structural charge that must be compensated by positively charged ions, K⁺ for natural muscovite. Upon adsorption of water, the K⁺ ions on the surface are hydrated by H₂O molecules. Whether washing with water replaces surface K⁺ with H₃O⁺ is a matter of ongoing discussion.^{1,2,16}

There have been several recent experimental and computational studies of direct significance to the results presented here. Miranda et al.¹² have proposed a stable ice-like structure on the hydrated muscovite (001) surface at room temperature based on sum-frequency-generation (SFG) vibrational spectroscopy and scanning polarization force microscopy (SPFM) experi-

* Address correspondence to this author.

† Department of Geology, University of Illinois at Urbana–Champaign.

‡ Current address: Geology Department, University of California at Davis, 166 Everson Hall, One Shields Avenue, Davis, CA 95616. Phone: (530) 754-8617. Fax: (530) 752-0951. E-mail: jwwang@ucdavis.edu.

§ NSF Water CAMPWS, University of Illinois at Urbana–Champaign.

§ Sandia National Laboratories.

mental data. A well-ordered 2-dimensional ice-like water structure on this surface has been proposed based on the results of ab initio molecular dynamics simulations.³ However, due to computational constraints, this ab initio MD simulation was very short (2 ps) and involved only two unit cells of the muscovite surface, which might not allow the calculations to sufficiently probe the phase space of the modeled system.³ Cheng et al.¹ have used synchrotron X-ray reflectivity measurements to determine the molecular density profile of water perpendicular to the muscovite (001) surface, and Park and Sposito² have used Monte Carlo (MC) computer simulations to model this profile. The interpretation of the experimental density profiles assumed complete exchange of H_3O^+ with surface K^+ ions, but the resolution of the experimental profiles is $\sim 1.1 \text{ \AA}$, and thus they may not resolve many details of the near-surface water structure.¹ In addition, the MC results do not address the contribution of K^+ to the total atomic density, because only the density of oxygen of H_2O ($\text{O}_{\text{H}_2\text{O}}$) was included in the comparison with the experimental total atomic density.² Cantrell and Ewing⁴ have used data from water adsorption isotherms on muscovite (001) to extract the enthalpy and entropy of adsorption as functions of water coverage. The results show that the condensation of water on the muscovite surface is exothermic at all coverages and that the enthalpy and entropy of adsorption have minima at approximately a monolayer coverage ($\theta = 1.0$).⁴ The adsorption enthalpy and entropy both increase and approach the respective bulk water values with increasing coverage ($\theta > 1.0$), but they also increase with decreasing coverage at $\theta < 1.0$.⁴ Molecular-level interpretation of the structure and dynamics of the adsorbed aqueous phase inferred from these experimental measurements remains largely speculative.

To better understand the molecular-scale structure, dynamics, and energetics of thin water films on the muscovite (001) surface, we have undertaken a series of MD simulations for different amounts of water on the surface at ambient conditions ($T = 300 \text{ K}$, $P = 0.1 \text{ MPa}$). The results show that H_2O molecules hydrate the muscovite (001) surface in a discrete way with specific adsorption sites at short distances from the surface. This site specificity is gradually lost at larger distances, and further hydration proceeds in a less structured manner. The MD-calculated atomic density profile for $\text{O}_{\text{H}_2\text{O}}$ is qualitatively consistent with the X-ray reflectivity data,¹ but our MD results also reveal a more detailed picture of the fluid structure near the interface, which could not be resolved by the experiment. The calculated hydration energy as a function of water coverage is also in good quantitative agreement with the measurements of hydration enthalpy⁴ except at the lowest coverages.

Methods

Structure and Models. The muscovite, $\text{KAl}_2(\text{Si}_3\text{Al})\text{O}_{10}(\text{OH})_2$, structure consists of aluminosilicate layers composed of two tetrahedral Si,Al sheets that are connected by an Al dioctahedral layer, forming so-called TOT layers, which are held together across the interlayer space by K^+ .^{14,19,20} The tetrahedral Al/Si ratio is 1/3, resulting in a negative structural charge that is compensated by interlayer K^+ . The long-range distribution of Si and Al on the tetrahedral sites is disordered, but the short-range ordering follows the Loewenstein Al-avoidance rule.^{21,22} The tetrahedral sheet consists of connected six-member rings. In the octahedral sheet, one of the two sites (M2) is occupied by Al and the other site (M1) is vacant. OH groups of the octahedral sheet are oriented about 74° to the normal to the sheet plane.²³ K^+ ions are coordinated to the bridging oxygen atoms, O_b , from the two adjacent tetrahedral sheets (Figure 1).

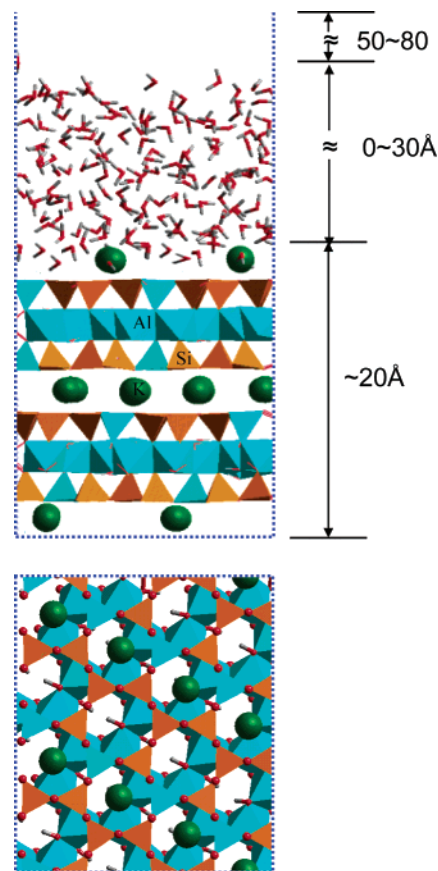


Figure 1. A schematic representation of the muscovite–water simulation models; x - z (top) and x - y (bottom) projections. The sticks are water molecules; the large balls are K^+ ions; the triangular polyhedra are Si,Al tetrahedra; other polyhedra are Al octahedra; small balls are bridging oxygens between Si,Al tetrahedra.

TABLE 1: Comparison of Crystallographic Cell Parameters from Experiment and MD Simulation

	experiment ¹⁴	MD calculation	deviation ($\pm\%$)
a axis (\AA)	5.202 ± 0.002	5.183 ± 0.012	-0.4
b axis (\AA)	9.024 ± 0.003	8.968 ± 0.028	-0.4
c axis (\AA)	20.078 ± 0.008	19.954 ± 0.079	-0.6
α angle (deg)	90.00	90.034 ± 0.093	+0.0
β angle (deg)	95.756 ± 0.006	95.643 ± 0.092	-0.1
γ angle (deg)	90.00	89.924 ± 0.049	-0.1

The monoclinic $C2/c 2M_1$ muscovite crystal structure¹⁴ was used as the initial input structure for our MD simulations. NPT -ensemble MD simulation of bulk muscovite without any symmetry constraints ($P1$), using the CLAYFF force field²⁴ at ambient conditions ($T = 300 \text{ K}$, $P = 0.1 \text{ MPa}$), reproduces the experimental crystal structure well, yielding the unit cell a , b , and c dimensions within 0.6% of the experimental values¹⁴ (Table 1). The calculated angles α , β , and γ are also close to the observed values¹⁴ (Table 1), and the stacking of adjacent TOT layers is well reproduced. Across the interlayer, the bridging oxygen atoms (O_b) of one TOT layer lie directly above those of the neighboring one, as in the experimental structure.^{14,20} Each K^+ ion is in the center of the interlayer space between two TOT layers and at the center of the upper and lower Al/Si di-trigonal six-member tetrahedral rings that coordinate it. The OH groups in our model remain almost parallel to the layer plane and point toward the vacant octahedral site, as expected for dioctahedral sheet silicates.

For simplicity, all tetrahedral Al atoms in our muscovite model were arranged in an ordered fashion. In each tetrahedral sheet, half of the six-member rings have the composition

Si_4Al_2 , the other half have Si_5Al_1 , and no $\text{Al}[4]-\text{O}-\text{Al}[4]$ bonds are allowed. To reduce the distortion of the Al octahedra, the tetrahedral Al sites were arranged such that only one of the oxygen atoms of an octahedron is bonded to a tetrahedral Al. For bulk muscovite, each K^+ ion was located between one Si_4Al_2 six-member ring and one Si_5Al_1 six-member ring to evenly distribute the charge.

The model muscovite surface was built by cleaving the muscovite structure along the (001) plane at the middle of the interlayer space. After cleavage, each surface retained half of the interlayer K^+ ions, and each of these was placed above the Si_4Al_2 di-trigonal rings, resulting in lower total computed energy than if some were above the Si_5Al_1 six-member rings. This K^+ position is confirmed by the results of ab initio calculations.³ The orthogonal x and y dimensions of the model surface are respectively $4 \times a$ and $2 \times b$ of the unit cell dimensions computed in the test MD runs with bulk crystalline muscovite. Thus, the muscovite surface in the computational supercell consists of 8 unique surface unit cells, and each simulated surface contains 48 bridging oxygen atoms and 8 K^+ (or, in some simulations, H_3O^+ ; Figure 1). The z direction of the simulation supercell coincides with c^* of the bulk crystal, and its total size was 100 Å, resulting in a separation between adjacent surfaces of at least 50 Å. This separation effectively eliminates the influence of one surface on the water adsorbed on the other (upper part of Figure 1). The final rectangular simulation supercells have x , y , and z dimensions of 17.79 Å \times 20.73 Å \times 100 Å, respectively. Periodic boxes with the same x – y dimensions and containing a variable number of H_2O molecules at a liquid water density of 1.0 g/cm³ were prepared in separate MD simulations of bulk water and were then inserted between the muscovite layers in contact with the surfaces. The coverage (θ) of water molecules on the surfaces is defined as the ratio of the total number of water molecules in the model system to the number of bridging oxygen atoms on the muscovite surface.⁴ $\theta = 1.0$ is a good estimate of a full monolayer of surface H_2O molecules having approximately a bulk liquid water density at ambient conditions. Six different models were constructed with the number of water molecules varying from 0 to 319 resulting in coverages with $\theta = 0.0, 0.31, 0.83, 1.63, 3.38, \text{ and } 6.65$.

MD Simulations. MD simulations were undertaken using methods and algorithms previously described.^{25–31} Three-dimensional periodic boundary conditions were applied, and all energy expressions and interatomic interaction parameters were taken from the CLAYFF force field.²⁴ Partial atomic charges in this force field are derived from periodic density functional calculations for a series of well characterized model compounds, and non-Coulomb interactions are described by conventional Lennard-Jones (12-6) functions. For water molecules, the flexible version of the simple point charge (SPC) potential was used.^{32,33} This potential has been thoroughly tested in numerous molecular simulations of aqueous systems.^{34–39} Potential parameters for the hydronium ion, H_3O^+ , consistent with the SPC water model, were taken from the literature.^{40,41}

The x and y supercell dimensions were slightly adjusted in a series of preliminary calculations for bulk muscovite to achieve the desired pressure for the final equilibrium MD simulations. These preliminary calculations consisted of energy minimization, followed by 50 ps MD runs at constant volume and $T = 300$ K and, finally, by 100 ps MD runs at constant $T = 300$ K and $P = 0.1$ MPa. The last 100 ps of the trajectories resulting from these *NPT* MD simulations were then used to determine the densities and supercell dimensions of the final equilibrium MD

simulations. Further structural relaxation of each model containing water molecules with these predetermined supercell parameters was achieved in four stages. First, the positions of all atoms in the substrate were fixed, and only the positions and orientations of H_2O molecules and surface K^+ (or H_3O^+) ions were allowed to relax in an energy minimization procedure. This was followed by a relatively short (10–50 ps) *NVT*-ensemble MD run. Then the atoms in the substrate were released, and in the last two stages the energy minimization and MD steps were repeated with all atoms of the system free to relax.

These optimized structures were then used as the starting configurations for the final MD simulations, which were all performed in the *NVT*-ensemble. Since all atoms in each system were completely free to move during these simulations, the constant-volume modeling approach with a fixed cell shape does not introduce significant limitations on the resulting interfacial structure, dynamics, and energetics of water. A time step of 1.0 fs was used for all MD simulations, and each system was allowed to equilibrate for 500 ps of MD simulation. The equilibrium dynamic trajectory for each model was finally recorded for statistical analysis at 10 fs intervals during the next 500 ps of MD simulation.

Simulation Analysis. Atomic density profiles in the [001] direction perpendicular to the solid surface were calculated by averaging over the last 500 ps equilibrium MD trajectory for each system. The planes defined by the average positions of the surface bridging oxygen atoms of muscovite were taken as the origin ($z = 0$). Atomic density maps within the planes parallel to the surface were also computed for each atom type in the system at variable distance from the surface for each simulation. Three angular variables, φ_D , φ_{HH} , and φ_N , are used to describe the orientation of each H_2O molecule with respect to the surface. They are defined by the angles between the surface normal direction [001] and respectively the dipole vector (\mathbf{v}_D , nearly parallel to the bisector of the H–O–H angle and positive from the O- to the H-end of the molecule), the H–H vector (\mathbf{v}_{HH}) from one hydrogen atom to the other, and the normal (\mathbf{v}_N) to the H–O–H plane of each water molecule. The orientations of all H_2O molecules were computed at 10 fs intervals from saved trajectories, and the angular distributions of these three angles were calculated as functions of distance from the muscovite surface. The local structural environment of the adsorbed water molecules was characterized by the nearest neighbor coordination number, the instantaneous number of H-bonds donated and accepted by each individual water molecule, and the fraction of H_2O molecules with specific numbers of H-bonds (distribution of H-bonding states). The detailed definitions and analyses of these parameters are described elsewhere.^{25,28}

The self-diffusion coefficients of H_2O molecules in the bulk liquid state and on the muscovite surfaces were calculated from the mean-square displacement of the oxygen atoms of H_2O . Statistical errors of these calculations are approximately 10–15%. For the muscovite–water systems, the diffusion coefficients along the z direction and within the x – y plane were estimated separately from the respective components of the diffusion tensor.

The energy of surface hydration, $U_{\text{H}}(N)$, was calculated using the formula:

$$\Delta U_{\text{H}}(N) = [\langle U(N) \rangle - \langle U(0) \rangle] / N \quad (1)$$

where N is the number of water molecules, $\langle U(N) \rangle$ is the average potential energy of an equilibrium system with N water molecules on the surface, and $\langle U(0) \rangle$ is the average potential

energy of an equilibrated dry surface used here as a reference hydration state.⁴² The hydration energy calculated in this way is a convenient and useful parameter for predicting relative thermodynamic stability of hydrated layered materials. For comparison of the calculated hydration energies with experimentally measurable enthalpies of hydration, we assume that the $P\Delta V$ term can be safely neglected, because it is small at ambient pressures. Whitley and Smith⁴³ have recently demonstrated that entropic effects likewise play only a relatively small, compensating role in the calculation of free energies of hydration and swelling of hydrous phyllosilicate phases.

The criteria used here to define the existence of a hydrogen bond are those frequently used in the analysis of bulk liquid water structure: intermolecular $O\cdots H$ distances less than 2.45 Å and angles, β , between the $O\cdots O$ and $O-H$ vectors less than 30° .⁴⁴ Oxygen atoms of the muscovite surface are treated in the same way as O_{H_2O} (as potential H-bond acceptors) for the purpose of hydrogen bonding calculations. The threshold of $R_{O\cdots H} \leq 2.45$ Å is used because it corresponds to the first minimum of the $O-H$ radial distribution function for the SPC water model in bulk liquid state under ambient conditions. $\beta \leq 30^\circ$ is chosen because it covers 90% of the angular distribution of H-bonds in bulk liquid water under the same conditions.^{44,45} These criteria are also consistent with the most recent direct X-ray adsorption spectroscopic measurements of the first hydration shell of H_2O in bulk liquid.⁴⁶

Results and Discussion

Density Profiles and Comparison with X-ray Reflectivity Measurements and MC Simulations. The density profiles for the oxygen and hydrogen atoms of H_2O molecules (O_{H_2O} and H_{H_2O}) provide the basis for understanding how the structure of interfacial water is affected by the presence of a muscovite surface and by a vapor phase on the opposing side of the aqueous film (Figure 2a,b). For O_{H_2O} (Figure 2a), the shapes and positions of the first two peaks are very similar at all water coverages, except that the first peak position at $\theta = 0.31$ is shifted away from the surface by about 0.3 Å. The peaks at larger distances from the surface remain essentially unchanged with increasing water film thickness. At the largest coverages, the O_{H_2O} density profiles exhibit five distinct peaks at about 1.7, 2.7, 3.6, 5.4, and 6.3 Å, and a broad, asymmetric peak between 8 and 11 Å. Smaller variations in atomic density extend to longer distances up to 15 Å from the surface.

At the liquid–vapor interface, the O_{H_2O} density increases from essentially 0 in the vapor to a value about 3% greater than the bulk-liquid value over a distance of about 5 Å and then decreases slightly to near the bulk value over about 1 Å. The 6 Å length over which the density changes associated with the vapor–liquid interface take place is typical of hydrophobic interfaces.^{47–52}

As observed for O_{H_2O} , the peak positions and shapes of the H_{H_2O} density profiles do not change greatly with increasing water film thickness (Figure 2b). At the largest coverages, the H_{H_2O} density profiles have five peaks at 1.2, 1.7, 2.9, 4.2, and 6.7 Å, and an asymmetric broad peak between 8 and 11 Å with no significant variation at distances greater than about 15 Å from the surface. The H_{H_2O} density variation at the vapor–fluid interface is very similar to that of O_{H_2O} .

The unequal spacings between maxima in the O_{H_2O} and H_{H_2O} density profiles indicate that the interaction between the muscovite (001) surface and adsorbed H_2O molecules is more complex than one would expect from simply the excluded volume effects of molecular packing at a solid interface.^{53,54} These “excluded volume” or “hard wall” effects result in a

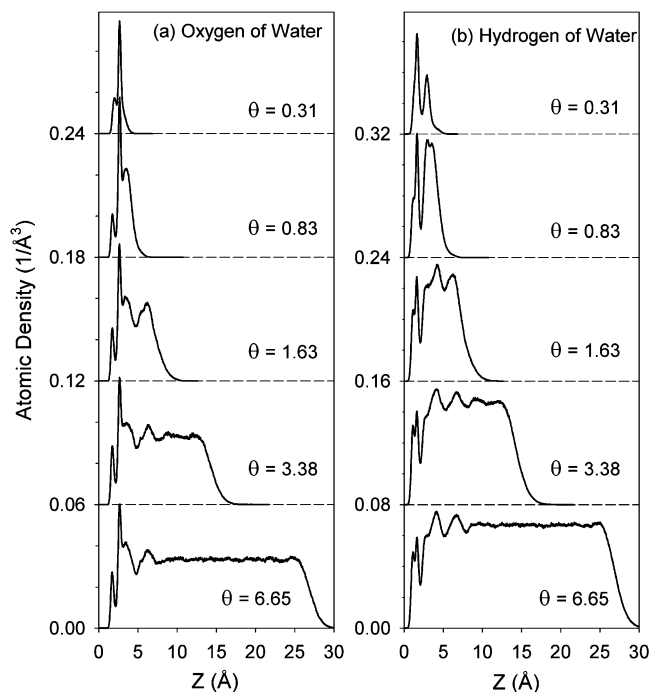


Figure 2. MD computed atomic density profiles for water at the muscovite (001) surface. Curves are displaced vertically by 0.06 \AA^{-3} (oxygen atomic density) and 0.08 \AA^{-3} (hydrogen atomic density) to avoid overlap. The position of the surface (0.0 in these plots) is computed as the average position of surface bridging oxygen atoms. θ is the surface water coverage defined as the ratio of the total number of water molecules in the model system to the number of bridging oxygen atoms on the muscovite surface.

periodic near-surface density profile variation with a wavelength approximately equal to the molecular diameter.⁵⁴ Thus, hydrogen bonding between adsorbed water molecules and the muscovite surface must play an important role in controlling the near-surface water structure.^{25,55,56} Recent computational results indicate that the near-surface water structure is strongly dependent on substrate structure and composition. The O_{H_2O} atomic density profiles at the muscovite (001) surface described here are very different from those at other mineral surfaces, including brucite (001),²⁵ talc (001),⁵⁷ MgO (001),⁵⁸ and NaCl (100).⁵⁹

The computed K^+ density profile at muscovite surface has only one peak at all water coverages (Figure 3). This peak is located about 1.5 Å from the completely dehydrated surface ($\theta = 0.0$) and about 1.7 Å from the surface for simulations with some water present. This result is in reasonable agreement with ab initio density functional calculations that show an outward shift of 0.11 Å for K^+ when the muscovite surface is hydrated.³ Adsorption of water onto the dry surface results in ionic hydration forces between the K^+ and the polar water molecules that pull the K^+ ions outward. All surface K^+ ions are located on top of the di-trigonal holes in the six-member tetrahedral rings on the surface and remain there for the duration of all our simulations. This result indicates that the negatively charged surface interacts more strongly with K^+ than with water molecules, on which the H-atoms each bear a positive charge ($0.41|e|$ in the SPC model³²). The K^+ adsorption sites and their distance from the surface in our MD simulations are quite different from the results of recent Monte Carlo simulations² for the same system, which locate K^+ ions 2.1 and 2.5 Å from the surface as hydrated outer-sphere complexes. These results suggest that surface-adsorbed water molecules prevent K^+ ions from directly coordinating with the basal oxygens of the surface.² In contrast, the K^+ ions in our simulations are all

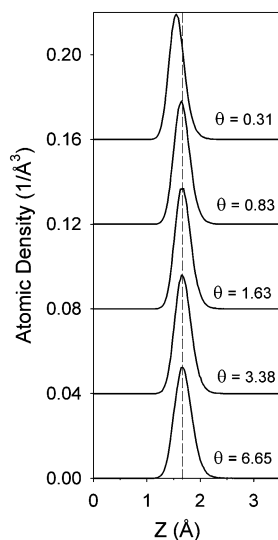


Figure 3. Computed atomic density profiles for surface K^+ ions. Curves are displaced vertically by 0.04 \AA^{-3} to avoid overlap.

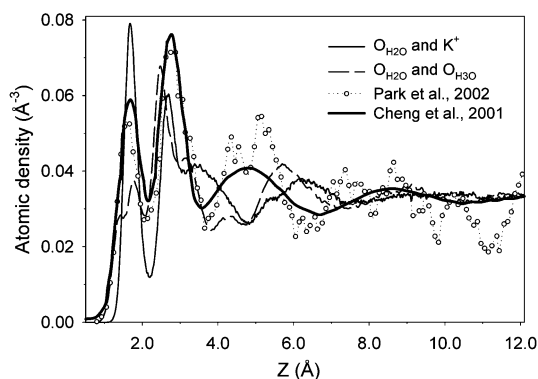


Figure 4. Comparison of water–oxygen density profiles. The thick solid line is the data from X-ray reflectivity experiments,¹ the circle-dotted line is the results from MC calculations,² the thin solid line is from our MD simulations plotting the combined density of K^+ and O of water, and the dashed line is from our MD calculation plotting the combined density of O of water and O of H_3O^+ ions. To provide a common origin for comparison, the experimental curve and that of MC calculations are offset 0.25 \AA in the positive z direction from the published distance scale.

coordinated to the basal oxygens in much the same way they are in the muscovite interlayer and occur at essentially the same distance as the water molecules contributing to the first peak of the water density profile (1.7 \AA ; Figure 3). This disagreement may arise from differences in the force fields used in the two sets of simulations, and may be resolvable by X-ray reflectivity experiments with higher resolution than currently available.

The total density profile from our MD calculations with the largest water coverage is qualitatively consistent with the results determined from experimental surface X-ray reflectivity measurements¹ and calculated from MC simulations² but shows significantly more detail (Figure 4). This total atomic density profile includes the contributions from both O_{H_2O} atoms and K^+ ions. The position and integrated density of the first peak from our calculation is comparable with those of both the experimental results and the MC simulation, but our distribution is narrower than both (Figure 4). The combined density and peak position of the second and third peaks in our simulation are also in good agreement with the parameters of the second peak in the X-ray measurements and MC simulation.^{1,2} The combined density from our fourth and fifth peaks is comparable to the third peak of the measured density profile, but the position

is about 1 \AA further from the surface than in the experimental results. The calculated peak position is probably within the uncertainty of the experimental results, which have a resolution of about 1.1 \AA .¹ The broad peak at about 8.5 \AA from the surface in the experimental profile is reproduced at about 9.0 \AA in our simulation. To provide a common origin for comparison, the experimental curve in Figure 4 is offset 0.25 \AA in the positive z direction from the published distance scale, which is within the precision of the measured peak locations. The data from MC simulations² were also offset by 0.25 \AA in the positive z direction in addition to their original 0.2 \AA offset relative to surface zero position (the original offset direction was not reported).

Interpretation of experimental results, such as X-ray reflectivity, X-ray photoelectron spectroscopy (XPS), and scanning polarization force microscopy for muscovite surfaces often assumes that rinsing the surface with deionized water causes replacement of K^+ by H_3O^+ .^{1,16} The results of additional MD simulations carried out under the same conditions and with the same procedures as described above but with H_3O^+ replacing all surface K^+ do not significantly improve comparison with the experiment density profile.¹ Therefore our MD simulations do not rule out the possibility that the surface K^+ ions remain on the surface after washing. In the $(O_{H_2O} + O_{H_3O^+})$ density profile from this simulation (Figure 4), the H_3O^+ contributes to the atomic density centered at 1.4 and 2.5 \AA . The resulting density-averaged peak position for the 1.7 \AA peak and the shoulder at $\sim 1.4 \text{ \AA}$ (Figure 4) is comparable to the first peak in the experimental profile, the MC-simulated profile, and our MD simulations with K^+ . The integrated atomic density at the surface, however, is lower with H_3O^+ . Careful visualization of the MD trajectory from this simulation shows that some of the surface di-trigonal cavities are not occupied by either a water molecule or a hydronium ion at every instant, resulting in an average di-trigonal ring occupancy < 1 . This incomplete surface site occupancy is compensated by the presence of H_3O^+ further from the surface, suggesting that relative to K^+ , H_3O^+ interacts more strongly with water than with the surface. If this is the case, it is energetically unlikely that H_3O^+ can substantially replace K^+ on the surface. This incomplete adsorption of water and H_3O^+ on the di-trigonal surface sites suggests incomplete wetting of the muscovite (001) surface with hydronium as a charge balancing ion.

At larger distances from the surface, however, there is a good agreement between the average peak position and integrated density of the combined second and third peaks in our simulations with H_3O^+ and the second peak of the experimental profile. Replacing K^+ by H_3O^+ ions at the surface also gives a better agreement of the average peak position and the integrated density of our combined fourth and fifth peaks and the experimental third peak, with only about a 0.4 \AA difference toward larger distances. This compares to a 1.0 \AA difference with K^+ . The broad peak centered at 8.5 \AA is also better reproduced.

As suggested by the atomic density profiles from our MD simulations (Figure 4), significantly different structural changes should occur if the surface K^+ ions were replaced by hydronium ions. Although the size and structure of H_3O^+ and K^+ hydration shells are quite different,^{60–62} it seems unlikely that the actual amount of K^+ and H_3O^+ on the hydrated surface of muscovite can be reliably estimated from X-ray experiments alone. This is because the $K^+ - H_2O$ distance is very close to the $H_2O - H_2O$ and $H_3O^+ - H_2O$ distances in bulk solution.⁶³ A combination of X-ray reflectivity experiments¹ with improved spatial

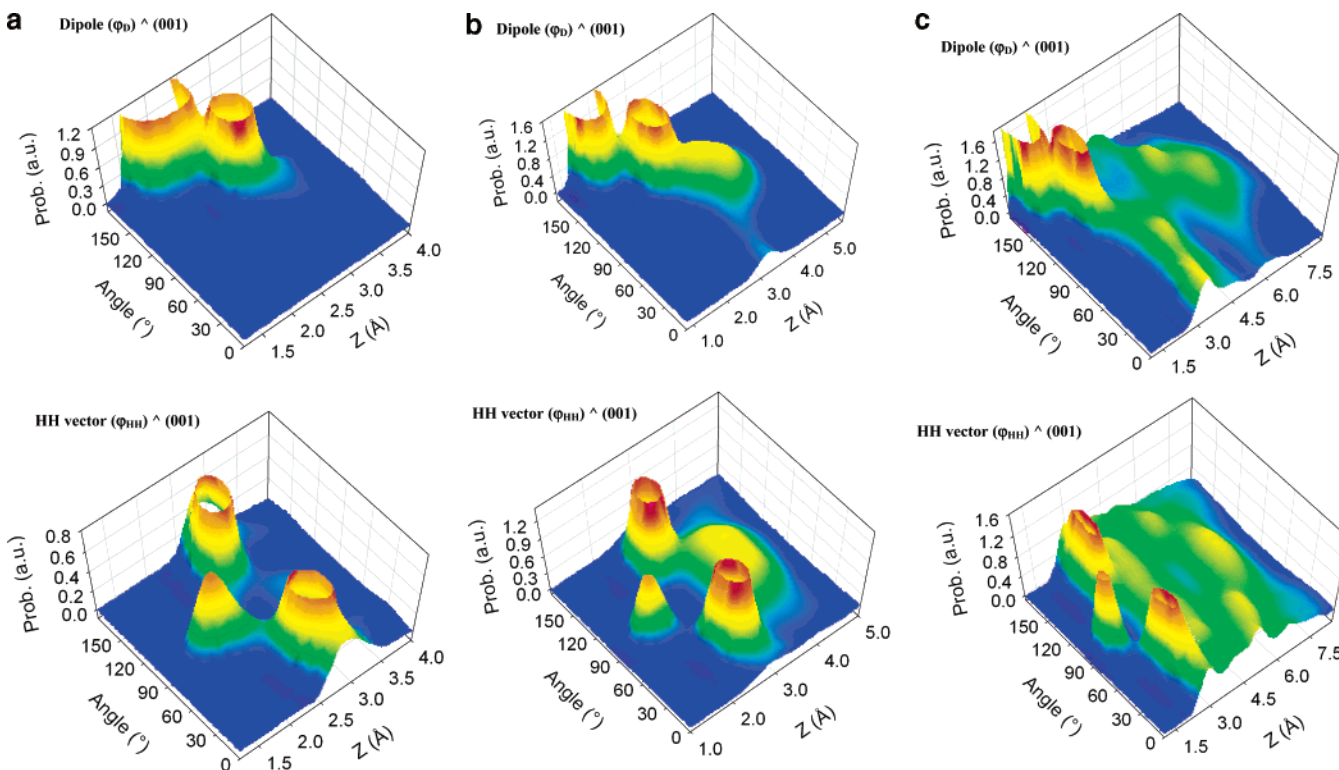


Figure 5. The angular distributions of H₂O orientation with distance from the muscovite (001) surface for adsorbed water molecules: (a) coverage $\theta = 0.31$, (b) coverage $\theta = 0.83$, (c) coverage $\theta = 1.63$. The top figures in parts a, b, and c are distributions of dipole \wedge [001], and the bottom figures are distributions of HH vector \wedge [001]. These angles are defined between the vectors and [001] direction. The probabilities were normalized by a sinusoid distribution. Thus, the integrals of each curve at any given distance from the surface are proportional to the number of water molecules at that distance.

resolution, H₂O orientation sensitive experiments (such as sum frequency vibrational spectroscopy⁶⁴ and infrared spectroscopy¹⁰), and molecular computer simulations could help to more accurately determine individual surface species and their contributions to the total experimentally observable atomic density profile.

Water Orientation. Unambiguous interpretation of the water structure at different distances from the surface is not possible from the density profiles alone, because a complete picture of water structure requires the information of surface H₂O orientation, nearest neighbor coordination, and the H-bonding. For muscovite, as for other phases previous examined,^{1,25,55,56} the water orientation at a given distance from the surface is not greatly affected by increasing water film thickness, paralleling the behavior in the density profiles. At a low surface water coverage of $\theta = 0.31$, the adsorbed H₂O molecules take on two different orientations corresponding to the first two peaks of the oxygen density profile (Figure 5a). The molecules at about 2.0 Å from the surface are predominantly oriented with $\varphi_D \sim 150\text{--}180^\circ$, $\varphi_{HH} \sim 70\text{--}90^\circ$, and $\varphi_N \sim 70\text{--}90^\circ$ (the third angular distribution is not shown in Figure 5a–c), whereas those at about 2.7 Å are predominantly oriented with $\varphi_D \sim 110\text{--}140^\circ$, $\varphi_{HH} \sim 20\text{--}50^\circ$, and $\varphi_N \sim 70\text{--}90^\circ$. For both types, the H₂O dipoles are oriented toward the surface. At a surface coverage slightly less than a monolayer ($\theta = 0.83$) the two groups of H₂O molecules observed at the lowest coverage are present, and a distinct liquid–vapor interface occurs at about 3.6 Å from the surface (Figure 5b). At $\theta = 1.63$ there are two additional groups of water molecules with different preferred orientations, corresponding to the third and fourth peaks in the oxygen density profile (Figures 2a and 5c). The molecules at 3.0–4.0 Å from the surface are predominantly oriented with $\varphi_D \sim 0\text{--}80^\circ$, $\varphi_{HH} \sim 30\text{--}90^\circ$, and $\varphi_N \sim 20\text{--}70^\circ$, and their dipoles point away

from the surface. The molecules at 4.5–5.5 Å are predominantly oriented with $\varphi_D \sim 100\text{--}140^\circ$, $\varphi_{HH} \sim 0\text{--}50^\circ$, and $\varphi_N \sim 70\text{--}90^\circ$, and their dipoles point toward the surface. At larger distances from the surface (6.5 to 10 Å), alternation of the dipole orientations continues, but the distributions are flatter. At even larger distances from the surface, where the oxygen density profile is essentially flat, water molecules can be found oriented with their dipoles pointing both away from and toward the surface (Figure 6), and these two orientations are mixed together at a given distance (10–12 Å). A completely flat, equal-probability orientational distribution of the angle φ_D is not observed in our simulations even at the largest coverage studied.

The calculated variation in the water dipole orientation with distance from the muscovite surface is clearly related to H-bonding between the water and the surface, H-bonding among water molecules, and the coordination of the K⁺ by water. The large negative structural charge of the surface plays a central role in this regard, and the presence of the liquid–vapor interface also has some effect. The orientation of the water dipoles pointing toward the surface in the first two layers defined by the O_{H₂O} density profile is expected due to the negative charge of the muscovite surface. The unexpected alternating orientation of H₂O molecules with dipoles pointing toward the surface and away from it is also principally related to the large surface charge. With a large net structural charge, the water molecules need to be oriented in a way to balance local charge. Therefore, at the muscovite (001) surface, the first two layers of water molecules are oriented with their dipoles predominantly pointing to the surface. These oriented water molecules induce a local electrostatic field that aligns the next layer of water molecules to be oriented with their dipoles pointing away from the surface. This is in striking contrast to the behavior of water at the neutral surfaces of brucite,²⁵ MgO,⁵⁸ and talc.⁵⁷ In the case of talc, water

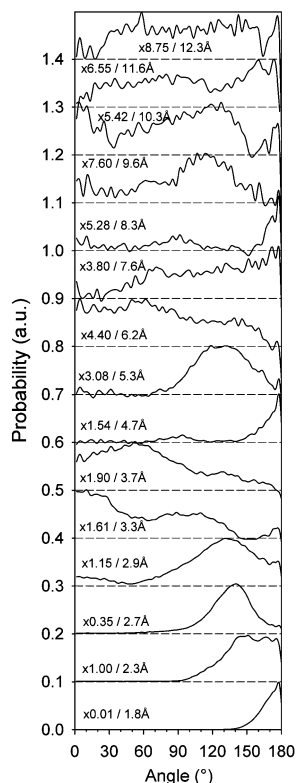


Figure 6. The distributions of the angle between the water dipole and [001] at coverage $\theta = 6.65$ at the indicated distances from the surface. Each curve was normalized as in Figure 5, rescaled individually, and displaced vertically by 0.1 to fit the figure. Note that the scaling used for plotting x is different at different distances from the surface.

dipoles pointing both toward and away from the surface occur in the first peak of the density profile.

A well-defined vapor–liquid interface forms at surface water coverages $\theta \geq 0.83$ (Figures 2, 5, and 6). The orientational distributions within this interface are similar for each system and independent of θ . At the distances corresponding to the maxima in the O_{H_2O} density profiles where the density begins to drop toward the vapor (such as at 25 Å for $\theta = 6.65$; Figure 2a), the H_2O molecules are predominantly oriented with $\varphi_D \sim 60\text{--}120^\circ$, $\varphi_{HH} \sim 60\text{--}90^\circ$, and $\varphi_N \sim 0\text{--}30^\circ$, that is with their dipoles essentially parallel to the vapor–liquid surface. This orientation is typical of water molecules at hydrophobic surfaces, where the molecules have stronger interaction with each other than with the surface. This orientation maximizes the total number of H-bonds with other water molecules. Within the ~ 5 Å interval near the vapor surface where O_{H_2O} density decreases significantly (such as from 27 to 29 Å for $\theta = 6.65$; Figure 2a), most H_2O molecules are oriented with $\varphi_D \sim 50\text{--}100^\circ$, $\varphi_{HH} \sim 0\text{--}30^\circ$, and $\varphi_N \sim 50\text{--}90^\circ$, i.e., with their molecular planes nearly perpendicular to the surface. This configuration is consistent with the results of SFG vibrational spectroscopy^{51,52} that indicate the existence of a significant number of water molecules having free (not H-bonded) OH groups at the liquid–vapor interface.

Hydrogen Bonding and Nearest Neighbor Coordination.

The specific features of the density profiles and orientational distributions of the near-surface water molecules described above are the result of interactions between these water molecules and the muscovite substrate and among water molecules themselves, with H-bonding playing a significant role in developing the local structure and nearest neighbor (NN) coordination of water. Our MD simulations show that the average number of H-bonds per H_2O molecule decreases from

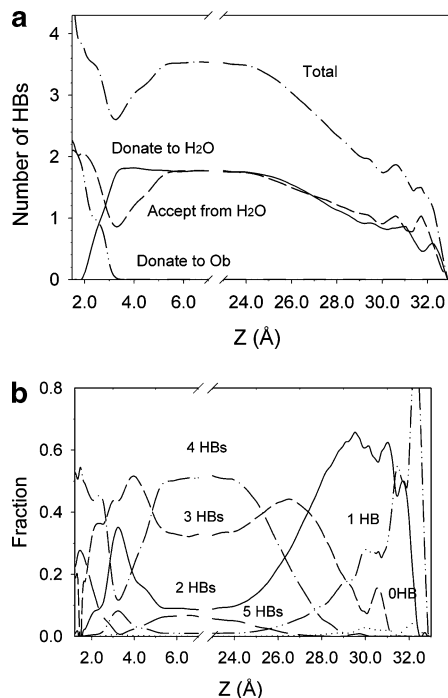


Figure 7. (a) Variation of the average total H-bond number per water molecule and the contributions of various H-bond types to this number with distance from the surface for the system at coverage $\theta = 6.65$. (b) Variation of the average fraction of water molecules with different numbers of H-bonds with distance from the surface for the system at coverage $\theta = 6.65$.

about 4.2 in the near-surface water layer to 3.5 (approximately the value for bulk liquid water simulated using the same SPC model) at distances ~ 10 Å from the surface. There is significant oscillation in this value within about 7 Å of the liquid–vapor interface. For water molecules contributing to the first peak of the oxygen density profile (Figure 2a), on average, each molecule accepts 2 H-bonds from other water molecules and donates 2 H-bonds to surface bridging oxygens, resulting in total about 4 H-bonds for each molecule at the surface (Figure 7a). Although this average value is similar to that of an ice-like H-bond structure,^{65–67} different water molecules in this group have different numbers of H-bonds and the average value is a statistical average of a dynamic picture. About 50% of the molecules participate in 4 H-bonds, 30% participate in 5 H-bonds, and 20% participate in 3 or fewer H-bonds at any instant (Figure 7b). This is quite different from the ice-like hydrogen bonding structure, where all molecules participate in 4 H-bonds. The difference in nearest neighbor coordination is even more striking. On average, each surface water molecule has 9 nearest neighbors, 6 surface O_b , and 3 other H_2O molecules (Figure 8). This high coordination occurs because each water molecule is located above the center of a six-member tetrahedral ring and donates H-bonds to two different O_b . In addition, each molecule accepts two H-bonds from two other neighboring water molecules that are located slightly further from the surface. There is also one additional nearest neighbor water molecule that typically does not form an H-bond with the central molecule. This instantaneous picture of local hydrogen bonding and nearest-neighbor coordination is consistent with the orientational distributions of surface H_2O molecules described in the previous section showing orientation of the dipoles of these molecules toward the surface. This structural arrangement is locally asymmetric and much different from any of the ice phases.

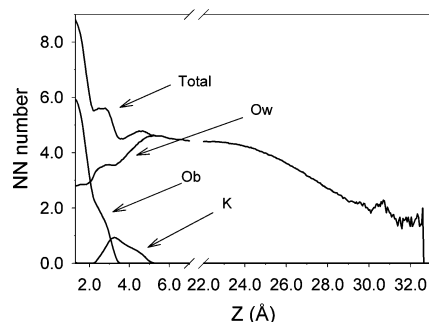


Figure 8. Variation of the average water coordination number and the contributions to this total with distance from the surface at coverage $\theta = 6.65$. Cut-off distances are 3.3 Å for O–O coordination and 2.45 Å for O–H coordination.

Water molecules at about 2.6 Å from the surface, corresponding to the second peak in the $\text{O}_{\text{H}_2\text{O}}$ density profile, accept on average ~ 1.5 H-bonds from other H_2O molecules, donate ~ 1 H-bond to surface oxygens, and donate ~ 1 H-bond to other water molecules (Figure 7a). This results in a total of 3.5 H-bonds per each water molecule, and 10% of them have 5 H-bonds, 40% have 4 bonds, 40% have 3 bonds, and 10% have 2 bonds (Figure 7b). This group of molecules has on average ~ 5.5 nearest neighbors consisting of ~ 1 surface oxygen, ~ 3.5 water molecules, and slightly less than 1 K^+ ions (Figure 8).

At distances of about 3.6 Å from the surface, corresponding to the third peak in the $\text{O}_{\text{H}_2\text{O}}$ density profile, each water molecule donates ~ 1.8 H-bonds to other water molecules and accepts ~ 1 H-bond from other molecules (Figure 7a), for a total of 2.8 H-bonds per molecule. About 15% of these molecules have 4 H-bonds, 50% have 3 H-bonds, 30% have 2 H-bonds, and 5% have 1 H-bond (Figure 7b). These molecules are too far from the surface to donate H-bonds to it and have, on average, ~ 4.5 nearest neighbors, ~ 3.5 H_2O molecules, and ~ 1 K^+ ions (Figure 8). These water molecules form the hydration shell of K^+ , and their dipoles are pointing away from the K^+ ions and away from the muscovite surface. In this orientation they are able to donate almost 2 H-bonds to other water molecules, but can accept only 1 H-bond, resulting in the minimum average number of H-bonds per water molecule at this distance from the surface as well as in the smallest fraction of molecules with 4 H-bonds.

At about 5.5 Å and further away from the surface, the water molecules are not coordinated to either surface bridging oxygen atoms or K^+ , and their local hydrogen bonding and coordination environments gradually change to closely resemble those of bulk liquid water at distances ≥ 8 Å (Figures 7 and 8).

At the liquid–vapor interface (best illustrated by the $\theta = 6.65$ results), there is a decrease in the number of H-bonds/water molecule beginning at about 25 Å from the surface. This decrease reflects the decreasing atomic density in this region as the water becomes more vaporlike. There is also a statistically noticeable difference in the number of donated and accepted H-bonds at about 25 Å from the surface (Figure 7a), where the local water density is 3% greater than in bulk liquid water (Figure 2a). This deficiency of accepted H-bonds is the direct result of the orientational change of these molecules and the gradual decrease of water density. At about 25 Å from the surface, the water molecules at shorter distances are oriented with their dipoles about 100° with the surface normal whereas those molecules at longer distances are oriented with their dipoles about 80° with the surface normal, resulting in the deficit of accepted H-bonds. There is a comparable deficiency of donated H-bonds at distances larger than 27 Å from the surface, where the water density is less than half the bulk value (Figures

2a and 7a). This deficiency indicates that there are a significant number of water molecules with acceptor-only or single-donor hydrogen bonding configurations in the interfacial region even at a relatively high average density. These two H-bonding configurations have been identified experimentally^{50–52} and in theoretical calculations.^{47–49} The results here provide added structural insight, however, because the experimental signals are averaged over a range of depths across the interface and do not resolve variations of H-bond configuration with depth in the interfacial region.

A more detailed hydrogen bonding analysis of the liquid–vapor interface shows that the total number of H-bonds and the fractions of water molecules having different numbers of H-bonds are strongly correlated with distance from the interface. The total number of H-bonds for each molecule gradually changes from the bulk value of ~ 3.5 to ~ 2.5 at about 27 Å from the surface and to ~ 2 at >29 Å from the surface. At these distances, the local density of water is sufficiently low (Figure 7a) to allow, on average, only one accepted H-bond and one donated H-bond for each water molecule, resulting in only two nearest neighbors (Figure 8). The fractions of H_2O molecules having a different number of H-bonds show systematic changes perpendicular to the interface (Figure 7b). The fraction of molecules with 4 H-bonds decreases continuously from 50% at 24 Å to nearly 0% at ~ 29 Å. The fraction having 3 H-bonds increases from 34% at 24 Å to a maximum of 45% at ~ 27 Å and then decreases to nearly 0% at ~ 31 Å. The fraction with 2 H-bonds has a maximum of $\sim 65\%$ at ~ 30 Å (about 1% of bulk liquid water density) and then rapidly decreases. The fraction with only one H-bond increases monotonically until the local water density becomes virtually zero (Figure 7b). It seems reasonable to conclude that the water molecules with 3 H-bonds contribute more to the single-donor signal and those with 1 or 2 H-bonds contribute more to the acceptor-only signal observed in the SFG vibrational spectroscopic studies.^{51,52}

Adsorption Sites and Surface Hydration. Water molecules hydrate the muscovite (001) surface by adsorbing to the lowest energy local environments available at a given surface coverage. At low coverage, the H_2O molecules can only probe the adsorption sites that are close to the surface, whereas at larger coverage with most of the lower energy sites occupied, water molecules can explore more adsorption sites at larger distances from the surface. It is convenient to describe the local atomic environment of adsorption sites using surface atomic density contour maps. These maps for adsorbed water close to the surface are practically independent of surface coverage, and thus only the results for $\theta = 6.65$ are reported and discussed below (Figure 9a–f).

In our simulations, all surface K^+ ions were initially placed above the Si_4Al_2 six-member ring cavities (Figure 9a), and none of them change their location during any of the 500 ps MD simulation runs at any surface coverage ($0.0 \leq \theta \leq 6.65$). Although the two most likely adsorption sites for K^+ (Si_4Al_2 rings and Si_5Al_1 rings) have only a small energy difference,³ the energy barrier to site hopping is large enough to make surface K^+ virtually immobile on the time scale of our MD simulations. This result is in contrast to the results of MC simulations,² which show K^+ ions displaced from the surface and almost all of the six-member ring cavities occupied by water molecules. Significant displacement of the K^+ from their surface sites seems quite unexpected, because the strong electrostatic attraction between the charged muscovite surface and K^+ ions should dominate the interaction between the surface and neutral water molecules. The electrical conductivity at the muscovite

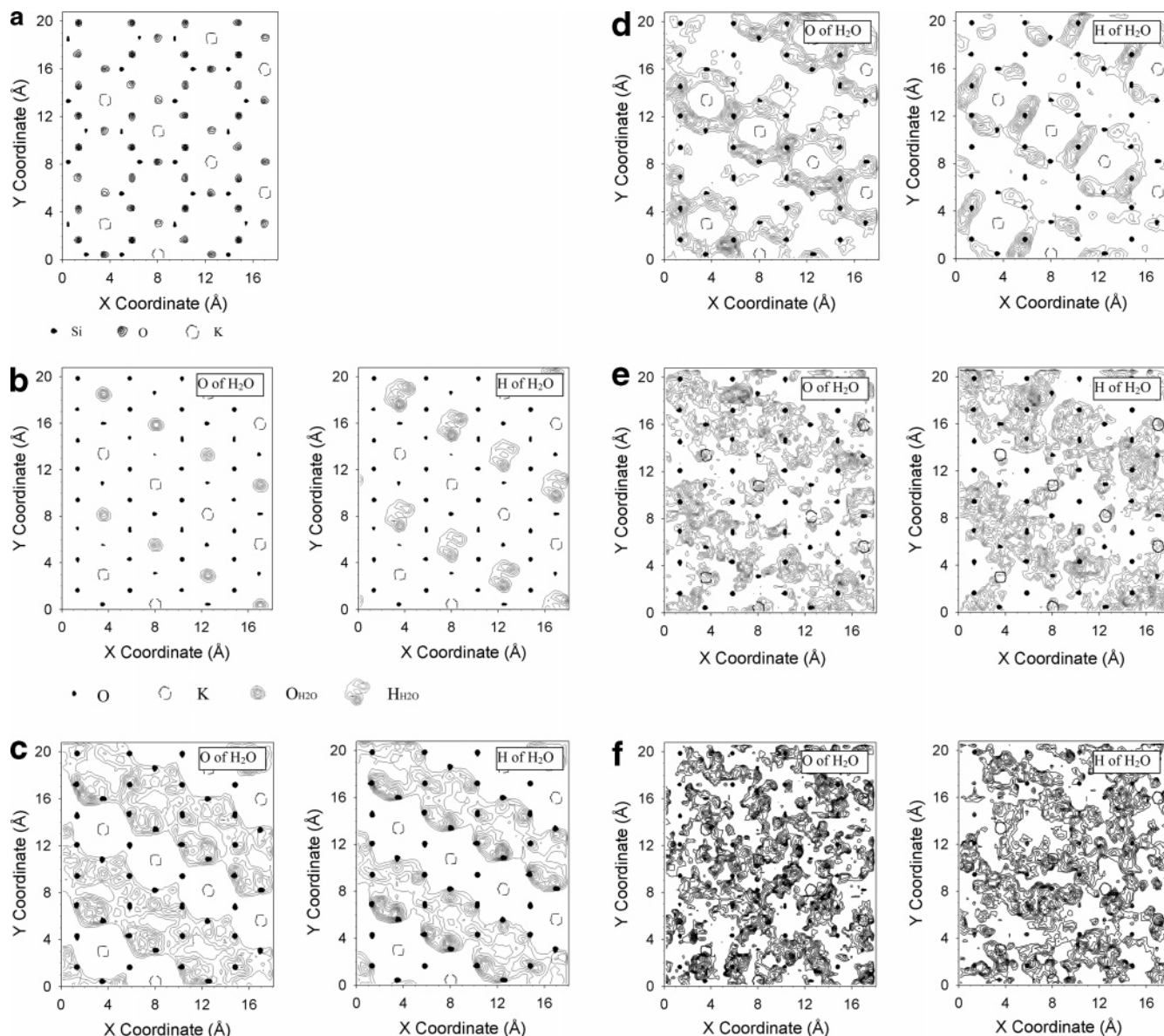


Figure 9. Atomic density contour maps for different species at the muscovite (001)–water interface. (a) Surface atoms of the muscovite (001) surface. Black dots are silicon atoms in the surface tetrahedral sheet, small thin line contours are surface bridging oxygen atoms, and large dashed line circles are surface K⁺ ions. (b–f) The density contour maps of water molecules within the first, second, third, fourth, and fifth peaks of water oxygen profiles (Figure 4), respectively. The black dots are surface bridging oxygen atoms, the large dashed circles are surface K⁺ ions, and the contours are oxygen density maps (left) and hydrogen density maps (right).

(001) surface increases significantly upon adsorption of water at monolayer coverage,⁶⁸ indicating increased mobility of surface K⁺ ions upon hydration. However, the time scale of this motion must be much longer than that of the motions discussed here.

In our simulations, all water molecules contributing to the first (1.7 Å) peak of the O_{H₂O} density profile occupy six-member ring cavities in which K⁺ is absent due to cleavage of the bulk muscovite crystal (Figure 9a,b). These H₂O molecules donate two H-bonds to the surface oxygens in the six-member rings (O_b). The average distance between surface oxygens and the oxygens of these water molecules is about 3.1 Å. This distance is within the range of hydrogen bonding (typically, <3.3 Å) and slightly longer than the average oxygen–oxygen distance in bulk liquid water. The average orientation of these molecules is slightly tilted, with the dipole oriented at 175° from the surface normal and the H-atoms oriented toward the Al[4] atoms substituting for Si[4] (Figures 5a and 9b). This orientation gives rise to the two density maxima in the H_{H₂O} map (Figure 9b). There is no apparent direct interaction among these molecules,

because they are more than 5 Å apart. The six-member ring cavity sites are one of the lowest energy sites (S2) suggested by a full structural optimization using ab initio methods,³ and they are also consistent with the MC calculations and X-ray reflectivity interpretations.^{1,2}

The water molecules contributing to the second (2.7 Å) peak of the O_{H₂O} density profile (Figure 4) find their energetically favorable adsorption sites around the water molecules in the six-member ring cavities (Figure 9c). There are six optimal adsorption sites located above each surface bridging oxygen atom and inside the six-member ring. Because of steric hindrance from neighboring water molecules, not every site can be simultaneously occupied. On average, each water molecule in this second layer donates 1/3 of an H-bond to other H₂O molecules within the layer, 2/3 of an H-bond to water molecules in the cavity (first layer), and 1 H-bond to surface bridging oxygens (Figure 7a). This arrangement results in an average perpendicular orientation of the molecular H–O–H planes of these molecules with respect to the surface and an average angle

of $\sim 130^\circ$ between their dipole and the surface (Figure 5). These adsorption sites are similar in location and orientation to the O1 sites of the 2-D ice structure suggested by the ab initio MD simulations.³ Careful analysis of our MD trajectories reveals that water molecules at these sites are H-bonded to both the H₂O molecules in the cavity and to other, neighboring water molecules at the equivalent sites to their own. This adsorption site cannot exist if the cavity is not occupied by a water molecule, and this could be the reason this site was not suggested by the ab initio study of single molecule adsorption on muscovite.³ The water molecules adsorbed at the cavity thus change the topography of the potential energy surface in the surrounding region significantly enough to make new secondary surface sites available for adsorption.

The water molecules contributing to the third peak of the O_{H₂O} density profile are largely coordinated to the surface K⁺ ions (Figure 9d). There are six adsorption sites around each K⁺ ion, all located above the surface bridging oxygen atoms. This arrangement creates a 12-coordinated environment for K⁺ (6 surface oxygens and 6 hydrating water molecules). The actual density maxima of the oxygen atoms of water in the density map might be somewhat displaced because of the interaction with the neighboring molecules (Figure 9d). The H_{H₂O} density map for the H-atoms of these molecules shows less ordering in their positions than that of O atoms around K⁺ ions, and the H_{H₂O} are pointing away from the ions. A similar adsorption site, S1, was suggested from the ab initio full structural optimization,³ with H₂O on this site forming a direct H-bond with the surface oxygen underneath. However, in our calculations these water molecules are too far from the surface to be able to form such H-bonds. Their dipoles are more or less parallel to or pointing away from the surface (Figure 5c). This orientation and H-bonding configuration for water molecules within the third peak of the O-density profile suggest that these water molecules laterally hydrate surface K⁺ ions (Figures 5c, 7a, and 8) and thus cannot accept more than 1 H-bond per molecule (Figure 7a).

For the water molecules contributing to the fourth and fifth peaks of the O_{H₂O} density profile, the atomic density maps for both oxygen and hydrogen of H₂O (Figure 9e,f) indicate much less ordering than those for molecules closer to the surface. It is difficult to assign specific adsorption sites for these molecules. However, statistically meaningful adsorption patterns are still clearly present. The areas with higher hydrogen densities for molecules contributing to the fourth peak are located above the areas of higher oxygen density for the molecules contributing to the second peak (Figure 9c,e). The dipoles of the water molecules in both the second and fourth peaks point principally toward the surface, indicating H-bond donation from those in the fourth peak to those in the second peak. The H₂O molecules contributing to the fifth and third peaks are similarly related to each other by H-bonding, but their dipoles point away from the surface (Figure 9d,f).

The S3 water site directly above the K⁺ ions suggested from a full ab initio structural optimization³ is not occupied in our simulations, because all K⁺ ions are already 12-coordinated within a hexagonal prism, and additional water cannot coordinate to it. This K⁺ coordination environment is quite different from that in bulk aqueous solutions, where the coordination number is about 8, 30% smaller.⁶³

There are some noticeable differences between the results of our MD simulations using classical potential models and the earlier ab initio MD simulations.³ Of the S1, S2, and S3 adsorption sites for single H₂O molecules on the surface

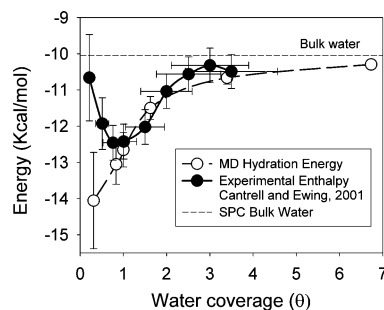


Figure 10. Comparison of experimental enthalpy and computed potential energy of water adsorption on the muscovite (001) surface. The filled circles and solid line are experimentally determined enthalpies of water adsorption, and the open circles and dashed line represent the surface hydration energy calculated from our MD simulations (eq 1).

suggested by the quantum calculations,³ only S1 and S2 are occupied in our MD simulations. Apart from obvious differences between classical and quantum approaches, another reason for this difference could be that the calculations for single molecular adsorption do not account for changes in the potential energy landscape seen by a molecule due to other water molecules located closer to the surface, such as at sites S1 and S2. That is, the presence of water on the surface changes the structural environment not probed by a single water molecule. Out of the sites composing the simulated 2-D ice structure,³ only the O1 site is occupied in our MD simulations, and a periodic H-bonding network representative of 2-D ice does not occur at any water coverage. Despite a noticeable slowing down of diffusional mobility at $\theta \approx 1$ (see the next section), the adsorbed water molecules in our simulations are, to a significant degree, structurally and orientationally more disordered at all water coverages.

The ab initio calculations³ were performed for a relatively small simulation cell containing only 2 surface unit cells and for a duration of only 2 ps. Both of these factors could have contributed to the enhanced tendency of the simulated surface structures to be periodically ordered and relatively stable. It is known that the H-bond lifetimes and H₂O reorientation times in bulk liquid water at ambient conditions are on the order of 2–5 ps^{44,63} and can be an order of magnitude longer for water molecules forming an ordered structure on a hydrophilic surface.⁶⁹ Thus, the ab initio MD simulations³ may have been able to probe only a relatively small region of the system's phase space and characterize only the vicinity of one of its local energy minima. If this was the case, the resulting structure would be significantly dependent on the initial arrangement of surface water molecules. In contrast, our classical MD simulations involve a surface area 4 times larger, and although we use an ordered arrangement of surface K⁺ ions to minimize local charge imbalance, the equilibrium simulations extended for 500 ps after an initial 500 ps equilibration period.

Hydration Energetics and Diffusive Dynamics of Interfacial Water. The hydration energies estimated from our MD simulations at more than a monolayer coverage are for the most part in good agreement with recent measurements of H₂O heats of adsorption on muscovite mica (Figure 10).⁴ This is the first attempt to compare computed and experimental values over a range of surface water coverages for this system. The calculated hydration energies increase monotonically from the lowest coverage ($\theta = 0.31$) to the highest coverage ($\theta = 6.65$), and at coverages $> \sim 3$ asymptotically approach the value characterizing the energy of individual water molecules in bulk SPC water. At $\theta \geq 1.0$, the simulated and experimental curves coincide within 0.5 kcal/mol, that is within the estimated errors for both

experimental and calculated values. Such a good agreement over a large coverage range indicates that our models correctly estimate the relative strengths of interactions between water and the muscovite surface and among the H₂O molecules themselves. This is a strong indication that the $P\Delta V$ term can be safely neglected for enthalpy calculations at more than a monolayer coverage under ambient conditions (low pressure). At coverages less than a monolayer ($\theta < 1.0$) (Figure 10), the difference between calculated and measured energies becomes large, and the difference increases with decreasing coverage. Indeed, the experimental values increase with decreasing coverage, whereas the calculated values decrease. Variation in the $P\Delta V$ term cannot explain this difference. At $\theta > 1$, we can approximate

$$P\Delta V = P[V_{\text{vapor}} - V_{\text{surface}}] \approx P[V_{\text{vapor}} - V_{\text{liquid}}] \quad (2)$$

which can only be neglected in comparison to the energy of hydration, ΔU_{H} (eq 1), if P is low enough (practically, close to or less than atmospheric pressure). On the other hand, at $\theta < 1$, we can assume that

$$V_{\text{surface}} \approx V_{\text{vapor}} \quad \text{or} \quad \Delta V \approx 0 \quad (3)$$

Thus, if the $P\Delta V$ term can be neglected at higher coverages because of very low P , there is even more reason to neglect it at lower coverages.

The discrepancy between the experimentally observed hydration enthalpies⁴ and the MD-calculated hydration energies at low surface coverages may be due to either experimental or computational effects. The MD simulations used the flexible SPC potential, and different water potentials may give different results.^{34,37,70–72} At low coverages, water molecules are more strongly perturbed by the surface than at larger coverages or in the bulk. Although the SPC model performs well for bulk water and overall seems to perform well for surface and confined water,²⁴ it may not perform as well at the muscovite (001) surface. MD simulations of water adsorption on the charge-neutral hydrophilic surfaces of gibbsite and brucite⁷³ show a slight increase of hydration energy at low coverages that are qualitatively similar to the experimental results for the muscovite (001) surface.⁴ Classical MD simulations using different potentials and more comprehensive ab initio MD simulations might resolve possible model-dependence problems. Experimentally, the discrepancy may be due to surface sorption of contaminants from the air, which might neutralize active surface sites and change the hydration energetics. The negatively charged, freshly cleaved muscovite (001) surface is extremely chemically active.¹⁷ Such surface contamination would most strongly affect the experimentally measured adsorption enthalpies at coverages $\theta < 1$, because under these conditions each H₂O molecule is adsorbed on the surface independently. If this were the case, $[\partial(\Delta U_{\text{H}})/\partial\theta]_{\theta < 1} \approx 0$, which is inconsistent with both the experimental and calculated values shown in Figure 10. Because the number of adsorbed water molecules is small at these coverages, the statistical errors for both sets of results are especially large in this range of θ , and a constant $\Delta U_{\text{H}} \approx -12.5$ kcal/mol probably satisfies both sets of data at $\theta < 1$.

The calculated self-diffusion coefficients of water on the muscovite (001) surface show that the total diffusion coefficient increases monotonically with increasing θ and also suggest that at all coverages the rate of diffusion is larger parallel to the surface than perpendicular to it (Figure 11). The diffusion coefficients are calculated from the mean-square displacement, and because of the bounding muscovite and vapor surfaces, the

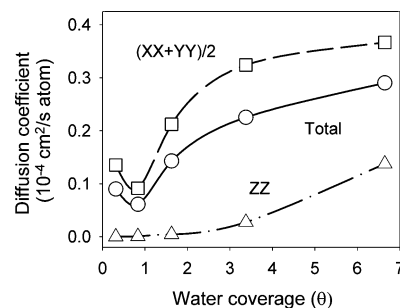


Figure 11. MD computed diffusion coefficients of oxygen of water molecules on the muscovite (001) surface. The filled circles and solid line are the total average diffusion coefficient, the open squares and dashed line are the average diffusion coefficient in the x – y plane, and the open triangles and dot dashed line are the average diffusion coefficient in the [001] direction.

distance a water molecule can move perpendicular to the surfaces is much more restricted than within the x – y plane. Diffusion coefficients calculated in this way are, thus, inherently lower at low coverage. The restricted diffusive motions in the z direction are compensated by enhanced mobility within the x – y plane, and our results show that the diffusion coefficient in the x – y plane is even larger than the total diffusion coefficient. (The total diffusion coefficient is not simply the average of the $xx + yy$ and zz components, because these do not capture translational correlations between directions.) A previously published MD study of water diffusion on the brucite (001) surface shows a factor of 1.5 increase of the self-diffusion coefficient in the x – y plane,⁷⁴ suggesting that such behavior may not depend greatly on the nature of the surface.

Our calculations also indicate that at $\theta < 1.0$ the water molecules are more mobile than at a full monolayer coverage (Figure 11), suggesting that water molecules are less constrained laterally at low coverages. This result is consistent with the calculated surface atomic density contour maps for $\theta = 0.31$, which indicate that almost all the water molecules are adsorbed in or near cavities in six-member rings, that they are clustered together (figure is not shown), that they occur on the sites of molecules contributing to the first two peaks of the density profiles at higher coverages, and that there is almost no H-bonding between these clusters. The atomic density maps at $\theta = 0.83$ show an H-bonding network connecting all the adsorbed water molecules and that cross-cluster hydrogen bonding stabilizes the adsorbed water molecules. This idea is also consistent with the suggestion that water molecules are more mobile at submonolayer coverages, as previously proposed on the basis of entropy calculations.⁴

Concluding Remarks

The MD simulations presented here as well as previous MC simulations and experimental X-ray reflectivity data^{1,2} show that water molecules within 10–15 Å of the muscovite (001) surface do not form a simple layered structure parallel to the surface with a periodicity approximately equal to the molecular diameter of 2.5 Å, as suggested by measurements using a surface force apparatus.⁷⁵ Rather, the surface structure, adsorption sites distribution, and the ability of the polar water molecules to orient at the surface are responsible for unequal spacing. Surface layering with equal spacing is typically observed only for nonpolar species or hydrophobic surfaces where the “excluded volume” or “hard wall” effects of molecular surface packing are dominant.^{53,54}

Our MD simulations indicate that water molecules on the muscovite (001) surface do not demonstrate a completely liquid-

like behavior, as otherwise suggested by the interpretation of X-ray reflectivity measurements¹ and MC simulations.² Their positions and orientations are more restricted than in bulk liquid water, and this structural ordering extends to larger distances from the surface than previously thought. Even at the largest coverage studied here ($\theta = 6.65$), over 20% of the water molecules are associated with specific adsorption sites, and another 50% have strongly preferred specific orientations with respect to the surface (Figure 6). Among previously studied surfaces, this partially ordered structure is unique to muscovite (001) and is different from any bulk ice-like structure. A well-ordered 2-dimensional ice-like structure, as suggested by ab initio MD simulations for $\theta = 1$,³ is also not observed in our simulations. Although the structure of the muscovite (001) surface has pseudohexagonal symmetry and the lattice constant is close to that of hexagonal ice, the H₂O molecular orientations at the surface are substantially influenced by H-bonding to the surface, surface charge distribution of the substrate, and the presence of the charge-balancing K⁺ cations on the surface. Both the surface structure and the orientations of the water molecules are important in the formation of an ordered ice-like phase.^{76,77}

Acknowledgment. This research was supported at the University of Illinois by Grant DEFGO2-00ER-15028 from the U.S. Department of Energy, Office of Basic Energy Sciences, Geosciences Research Program, and the NSF Center of Advanced Materials for Water Purification with Systems (Water-CAMPwS). Computation was partially supported by the National Computational Science Alliance (Grant EAR 990003N) and utilized NCSA SGI/CRAY Origin 2000 computers and the Cerius2-4.6 software package from Accelrys. Wang also acknowledges the fellowship from the University of Illinois at Urbana-Champaign. We also acknowledge Prof. Kathryn Nagy for fruitful discussions concerning the structure of water on muscovite, and Prof. George Ewing for invaluable comments and fruitful discussion. Cygan is appreciative of funding provided by the U.S. Department of Energy, Office of Basic Energy Sciences, Geosciences Research. Sandia is a multiprogram laboratory operated by Sandia Corporation, a Lockheed Martin Company for the United States Department of Energy's National Nuclear Security Administration under contract DE-AC04-94AL85000.

Supporting Information Available: Equilibrated structures and short trajectories from the MD simulations. This material is available free of charge via the Internet at <http://pubs.acs.org>.

References and Notes

- Cheng, L.; Fenter, P.; Nagy, K. L.; Schlegel, M. L.; Sturchio, N. *C. Phys. Rev. Lett.* **2001**, *87*, 156103.
- Park, S. H.; Sposito, G. *Phys. Rev. Lett.* **2002**, *89*, 085501.
- Odelius, M.; Bernasconi, M.; Parrinello, M. *Phys. Rev. Lett.* **1997**, *78*, 2855.
- Cantrell, W.; Ewing, G. E. *J. Phys. Chem. B* **2001**, *105*, 5434.
- Henderson, M. A. *Surf. Sci. Rep.* **2002**, *46*, 1.
- Menzel, D. *Science* **2002**, *295*, 58.
- Brown, G. E. *Science* **2001**, *294*, 67.
- Drever, J. I. *The geochemistry of natural waters—Surface and groundwater environments*, 3rd ed.; Prentice Hall: New York, 1997.
- Hochella, M. F.; White, A. F. *Rev. Mineral.* **1990**, *23*, 1.
- Ewing, G. E. *J. Phys. Chem. B* **2004**, *108*, 15953.
- Brown, G. E.; Henrich, V. E.; Casey, W. H.; Clark, D. L.; Eggleston, C.; Felmy, A.; Goodman, D. W.; Gratzel, M.; Maciel, G.; McCarthy, M. I.; Nealon, K. H.; Sverjensky, D. A.; Toney, M. F.; Zachara, J. M. *Chem. Rev.* **1999**, *99*, 77.
- Miranda, P. B.; Xu, L.; Shen, Y. R.; Salmeron, M. *Phys. Rev. Lett.* **1998**, *81*, 5876.
- Joseph, Y.; Ranke, W.; Weiss, W. *J. Phys. Chem. B* **2000**, *104*, 3224.
- Kuwahara, Y. *Phys. Chem. Miner.* **1999**, *26*, 198.
- Zhang, X.; Zhu, Y.; Granick, S. *Science* **2002**, *295*, 663.
- Xu, L.; Salmeron, M. *Langmuir* **1998**, *14*, 5841.
- Beaglehole, D.; Christenson, H. K. *J. Phys. Chem.* **1992**, *96*, 3395.
- Israelachvili, J. N.; Pashley, R. M. *Nature* **1983**, *306*, 249.
- McKeown, D. A.; Bell, M. I.; Etz, E. S. *Am. Mineral.* **1999**, *84*, 1041.
- Güven, N. Z. *Kristallogr.* **1971**, *134*, 196.
- Loewenstein, W. *Am. Mineral.* **1954**, *39*, 92.
- Brigatti, M. F.; Guggenheim, S. *Rev. Mineral. Geochem.* **2002**, *46*, 1.
- Beran, A. *Rev. Mineral. Geochem.* **2002**, *46*, 351.
- Cygan, R. T.; Liang, J.-J.; Kalinichev, A. G. *J. Phys. Chem. B* **2004**, *108*, 1255.
- Wang, J.; Kalinichev, A. G.; Kirkpatrick, R. J. *Geochim. Cosmochim. Acta* **2004**, *68*, 3351.
- Wang, J.; Kalinichev, A. G.; Amonette, J. E.; Kirkpatrick, R. J. *Am. Mineral.* **2003**, *88*, 398.
- Kirkpatrick, R. J.; Kalinichev, A. G.; Wang, J.; Hou, X.; Amonette, J. E. Molecular modeling of the vibrational spectra of interlayer and surface species of layered double hydroxides. In *The Application of Vibrational Spectroscopy to Clay Minerals and Layered Double Hydroxides, CMS Workshop Lectures*; Klopogge, J. T., Ed.; The Clay Minerals Society: Aurora, CO, 2005; Vol. 13, p 239.
- Kalinichev, A. G.; Kirkpatrick, R. J. *Chem. Mater.* **2002**, *14*, 3539.
- Wang, J. W.; Kalinichev, A. G.; Kirkpatrick, R. J.; Hou, X. Q. *Chem. Mater.* **2001**, *13*, 145.
- Cygan, R. T. *Rev. Mineral. Geochem.* **2001**, *42*, 1.
- Kalinichev, A. G.; Kirkpatrick, R. J.; Cygan, R. T. *Am. Mineral.* **2000**, *85*, 1046.
- Berendsen, H. J. C.; Postma, J. P. M.; van Gunsteren, W. F.; Hermans, J. Interaction models for water in relation to protein hydration. In *Intermolecular Forces*; Pullman, B., Ed.; Riedel: Dordrecht, The Netherlands, 1981; p 331.
- Teleman, O.; Jönsson, B.; Engström, S. *Mol. Phys.* **1987**, *60*, 193.
- Guillot, B. *J. Mol. Liq.* **2002**, *101*, 219.
- Robinson, G. W.; Zhu, S.-B.; Singh, S.; Evans, M. W. *Water in Biology, Chemistry and Physics. Experimental Overviews and Computational Methodologies*; World Scientific Publishing Co. Pte. Ltd.: Singapore, 1996; Vol. 9.
- Wallqvist, A.; Mountain, R. D. Molecular models of water: Derivation and Description. In *Reviews in Computational Chemistry*; Lipkowitz, K. B., Boyd, D. B., Eds.; Wiley-VCH: New York, 1999; Vol. 13; p 183.
- Jorgensen, W. L.; Chandrasekhar, J.; Madura, J. D.; Impey, R. W.; Klein, M. L. *J. Chem. Phys.* **1983**, *79*, 926.
- Mizan, T. I.; Savage, P. E.; Ziff, R. M. *J. Phys. Chem.* **1994**, *98*, 13067.
- Jorgensen, W. L.; Jenson, C. *J. Comput. Chem.* **1998**, *19*, 1179.
- Gertner, B. J.; Hynes, J. T. *Faraday Discuss.* **1998**, *110*, 301.
- Chialvo, A. A.; Cummings, P. T.; Simonson, J. M. *J. Chem. Phys.* **2000**, *113*, 8093.
- Smith, D. E. *Langmuir* **1998**, *14*, 5959.
- Whitley, H. D.; Smith, D. E. *J. Chem. Phys.* **2004**, *120*, 5387.
- Luzar, A. *J. Chem. Phys.* **2000**, *113*, 10663.
- Teixeira, J.; Bellissent-Funel, M.-C.; Chen, S.-H. *J. Phys.: Condens. Matter* **1990**, *2*, SA105.
- Wernet, P.; Nordlund, D.; Bergmann, U.; Cavalleri, M.; Odelius, M.; Ogasawara, H.; Näslund, L. Å.; Hirsch, T. K.; Ojamäe, L.; Glatzel, P.; Pettersson, L. G. M.; Nilsson, A. *Science* **2004**, *304*, 995.
- Patel, H. A.; Nauman, E. B.; Garde, S. *J. Chem. Phys.* **2003**, *119*, 9199.
- Kuo, I.-F. W.; Mundy, C. J. *Science* **2004**, *303*, 658.
- Wilson, M. A.; Pohorille, A.; Pratt, L. R. *J. Phys. Chem.* **1987**, *91*, 4873.
- Raymond, E. A.; Tarbuck, T. L.; Brown, M. G.; Richmond, G. L. *J. Phys. Chem. B* **2003**, *107*, 546.
- Du, Q.; Freysz, E.; Shen, Y. R. *Science* **1994**, *264*, 826.
- Du, Q.; Superfine, R.; Freysz, E.; Shen, Y. R. *Phys. Rev. Lett.* **1993**, *70*, 2313.
- Yu, C.-J.; Richter, A. G.; Datta, A.; Durbin, M. K.; Dutta, P. *Phys. Rev. Lett.* **1999**, *82*, 2326.
- Abraham, F. F. *J. Chem. Phys.* **1978**, *68*, 3713.
- Lee, S. H.; Rossky, P. J. *J. Chem. Phys.* **1994**, *100*, 3334.
- Spohr, E.; Hartnig, C.; Gallo, P.; Rovere, M. *J. Mol. Liq.* **1999**, *80*, 165.
- Bridgeman, C. H.; Skipper, N. T. *J. Phys.: Condens. Matter* **1997**, *9*, 4081.
- McCarthy, M. I.; Schenter, G. K.; Scamehorn, C. A.; Nicholas, J. B. *J. Phys. Chem.* **1996**, *100*, 16989.
- Stöckelmann, E.; Hentschke, R. *J. Chem. Phys.* **1999**, *110*, 12097.
- Laurs, N.; Bopp, P. *Ber. Bunsen-Ges. Phys. Chem.* **1993**, *97*, 982.
- Lee, S. H.; Rasaiah, J. C. *J. Phys. Chem.* **1996**, *100*, 1420.

- (62) Tuckerman, M. E.; Marx, D.; Klein, M. L.; Parrinello, M. *Science* **1997**, *275*, 817.
- (63) Ohtaki, H.; Radnai, T. *Chem. Rev.* **1993**, *93*, 1157.
- (64) Ostroverkhov, V.; Waychunas, G. A.; Shen, Y. R. *Phys. Rev. Lett.* **2005**, *94*, 046102.
- (65) Pauling, L. *J. Am. Chem. Soc.* **1935**, *57*.
- (66) Bernal, J. D.; Fowler, R. H. *J. Chem. Phys.* **1933**, *1*, 515.
- (67) Eisenberg, D.; Kauzmann, W. *The structure and properties of water*; Oxford University Press: Oxford, UK, 1969.
- (68) Beaglehole, D. *Phys. A* **1997**, *244*, 40.
- (69) Ruan, C.-Y.; Lobastov, V. A.; Vigliotti, F.; Chen, S.; Zewail, A. H. *Science* **2004**, *304*, 80.
- (70) Engkvist, O.; Stone, A. J. *J. Chem. Phys.* **2000**, *112*, 6827.
- (71) Vega, C.; Sanz, E.; Abascal, J. L. F. *J. Chem. Phys.* **2005**, *122*, 114507.
- (72) Jorgensen, W. L.; Tirado-Rives, J. *PNAS* **2005**, *102*, 6665.
- (73) Wang, J.; Kalinichev, A. G.; Kirkpatrick, R. J. *Geochim. Cosmochim. Acta* **2005**, in press.
- (74) Sakuma, H.; Tsuchiya, T.; Kawamura, K.; Otsuki, K. *Surf. Sci.* **2003**, *536*, L396.
- (75) Israelachvili, J. N.; Wennerström, H. *Nature* **1996**, *379*, 219.
- (76) Sadtchenko, V.; Ewing, G. E.; Nutt, D. R.; Stone, A. J. *Langmuir* **2002**, *18*, 4632.
- (77) Conrad, P.; Ewing, G. E.; Karlinsey, R. L.; Sadtchenko, V. *J. Chem. Phys.* **2005**, *122*, 064709.